FLIGHT SIMULATION ENVIRONMENTAL FATIGUE CRACK PROPAGATION IN 2024-T3 AND 7475-T761 ALUMINIUM

R.J.H. Wanhill
National Aerospace Laboratory
Amsterdam, The Netherlands

Abstract

Flight simulation fatigue crack propagation tests on 2024-T3 and 7475-T761 aluminium alloy sheet were carried out using a gust spectrum representative of the load history of an under wing skin in a transport aircraft. The investigation included tests at several design stress levels and in environments of laboratory air and air plus water spray. The results are discussed with respect to the choice of structural concepts using 7475 alloy and evaluation of the fatigue properties of such concepts.

Introduction

Aluminium alloys are the main structural materials for transport aircraft and are likely to remain so for at least another decade [1]. One of the most important design problems is whether 7000 series (Al Zn Mg Cu) alloys can be used to achieve weight savings in structures customarily made from 2000 series (Al Cu Mg) alloys while maintaining or improving the damage tolerance properties (safe crack growth life and fail-safety [2]). Recent studies have proposed using 7475 alloy sheet and plate instead of a 2000 series alloy (typically 2024-T3) for under wing skins and fuselage shells [3-5]. This proposal has its basis in the superior combinations of strength and fracture toughness possessed by 7475 [6]. However, with respect to fatigue crack propagation resistance 7475 appears usually to be inferior to 2024-T3 under constant amplitude and transport wing gust spectrum loading in laboratory air [6,7], and 7000 series alloys are known to be more sensitive than 2000 series alloys to changes in the environment [8].

The foregoing considerations led to definition of the present test programme, in which additional fatigue crack propagation data were obtained for 7475-T761 and 2024-T3 tested under gust spectrum loading at several design stress levels and in environments of laboratory air and air plus water spray. The purpose of using the air plus water spray environment was to simulate condensation on the still-cold airframe structure owing to transpiration during the descent phase of each flight [9].

The Gust Spectrum TWIST

TWIST (Transport WIng STandard) was established by the NLR and the Laboratorium für Betriebsfestigkeit (Darmstadt) and is fully described in [10]. For testing purposes the spectrum has been approximated by the stepped function shown in figure 1. Stresses are expressed non-dimensionally

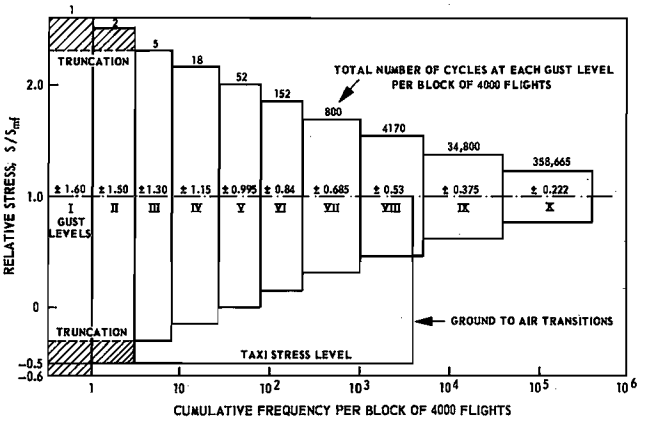

Fig. 1 The gust spectrum TWIST

TABLE 1

AVERAGE MECHANICAL PROPERTIES

material		0.2% offset yield stress (MPa)	UTS (MPa)	elongation on 50 mm (%)	elastic modulus (GPa)
2024-T3 Alclad	L	349	475	21	70.9
	T	307	461	22	72.3
7475-T761 bare	L	455	505	13	68.4
	T	448	512	13	69.3

by dividing them by the stress pertaining to undisturbed cruising flight, Smf. There are ten gust load levels and one taxi load level.

TWIST consists of blocks of 4000 different flights. There are ten different flight types, ranging from storm (A) to calm (J) conditions. The frequency of occurrence of each flight type and of each load level within each type of flight is reported in [7,10]. The load sequence was completed by defining the sequence of application of the different flights and the sequence of loads within each flight. Basic properties of the defined sequences are:

1) The flights and loads for each flight are applied in a random sequence except that clustering of severe flights is not allowed.

2) The loads within each flight are applied as a random sequence of half-cycles such that a positive half-cycle is followed by a negative half-cycle of arbitrary magnitude.

3) Load sequences have been generated individually for each flight. Thus flights of the same type generally have a different load sequence.

The positions of the severest flights in TWIST are: 1656 (type A); 2856 (type B); 501, 2936 and 3841 (type C).

The Test Programme

Materials

The materials were 3.1 mm thick 2024-T3 Alclad and 2.8 mm thick 7475-T761 sheet. These thicknesses are representative for transport aircraft under wing skin stiffened panels of end load capacity ~ 3 MN/m. Average mechanical properties are given in table 1: they are typical for these alloys.

Specimens

The specimens were centre-cracked panels 235 mm long in the rolling direction of the sheet and 150 mm or 160 mm wide. These differing widths were necessary owing to interfacing with other test programmes. Crack starter notches were 1.5 mm long jeweller's sawcuts at either side of a 4 mm diameter hole.

Test conditions and procedure

Mean stress levels, Smf, were 70 MPa for the 160 mm wide specimens and 80 and 95 MPa for the 150 mm wide specimens, and all other stresses were scaled according to the ratios given by TWIST with the gust load spectrum truncated to level III, figure 1. This level corresponds to 8 occurrences of maximum load in 4000 flights and is a reasonable truncation level for fatigue crack propagation testing [7].

The environments were laboratory air of 40 - 60% relative humidity and laboratory air plus a water spray of 0.35 weight % NaCl in distilled water. The air plus water spray environment was applied in the following way. Paint spray nozzles directed a continuous stream of air onto the specimen crack paths and a solenoid - actuated valve allowed a water spray through the nozzles for 2 seconds halfway through each simulated flight. The distance of the nozzles from the specimen and the relative amounts of air and water spray were adjusted until fine droplets formed on the specimen surface and dried up by the time the average simulated flight ended. The addition of salt, in a concentration one-tenth of that in seawater, was thought to be reasonable in view of the frequent availability of salt as a contaminant [11]. Ambient temperature for both environments was typically 295 K.

The specimens were tested in a 250 kN frame fitted to an MTS closed loop electrohydraulic machine. The closed loop system was controlled by an NLR-developed device, PAGE (Programmed Amplitude GEnerator). The TWIST load sequence was stored on magnetic tape and read by a KENNEDY incremental recorder.

All tests were begun at flight number 1. Buckling during compression loads was prevented by felt-lined aluminium alloy antibuckling guides which had cutouts for visual observation of the cracks. The specimens were tested in series of two. When one specimen failed it was replaced by a dummy specimen and the test continued to failure of the remaining specimen. The cycle frequency was 15 Hz in laboratory air and 5 Hz in the air plus water spray environment. These frequencies were chosen because a test frequency of 15 Hz in air is likely to give the same result as a real time test [8], and a frequency of 5 Hz in air plus water spray represents a compromise between the need to minimise testing time and allowing sufficient time for environmental effects.

Results

Crack propagation lives and life ratios

Figure 2a shows the crack propagation lives of 2024-T3 and 7475-T761 specimens as functions of mean stress level, Smf, and environment. The lives have been taken from initial total crack lengths

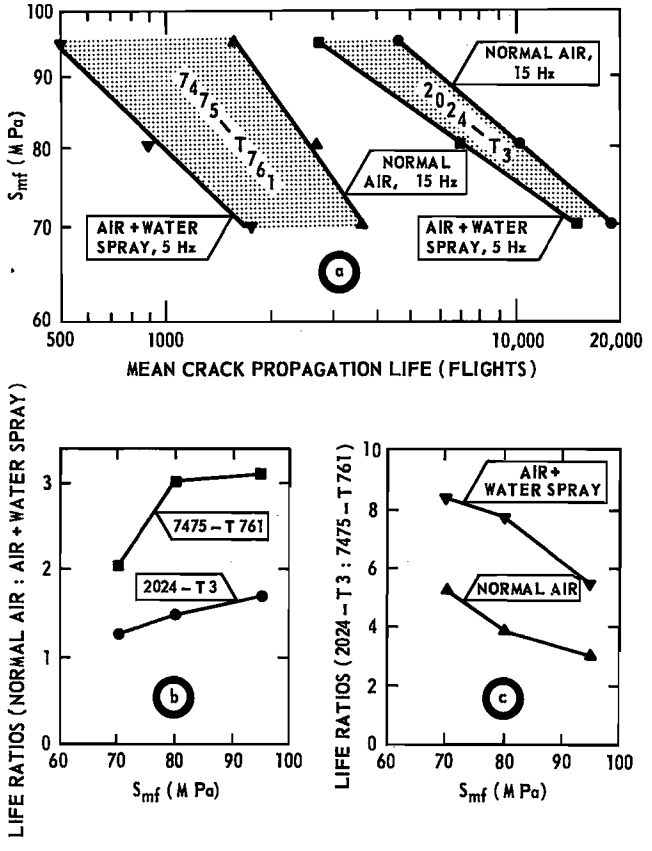

Fig. 2 Crack propagation lives and life ratios

of 9 mm for 150 mm wide specimens (Smf = 80 and 95 MPa) and 9.6 mm for 160 mm wide specimens (Smf = 70 MPa). 2024-T3 specimens had much longer lives than 7475-T761 specimens, especially at lower stress levels.

Figures 2b and 2c give crack propagation life ratios and show that:

1) For both materials the sensitivity to changing the environment increased with increasing Smf.

2) 7475-T761 was more sensitive to changing the environment.

3) For both environments the relative performance of 7475-T761 to that of 2024-T3 was worse with decreasing Smf.

4) The relative performance of 7475-T761 to that of 2024-T3 was significantly worse in air plus water spray.

In general, the effect of changing from an environment of normal air to air plus water spray was fairly strong, since life ratios in figure 2b are as high or higher than those found for 2024-T3 and 7075-T6 specimens tested continuously in 3.5% aqueous NaCl and in normal air [12]. The strong effect in the present test series can be attributed in part to two experimental observations:

1) The fatigue cracks contained water during most of the duration of tests with air plus water spray, even though the specimen surfaces regularly dried.

2) Salt deposited on the specimen surfaces near the cracks and liquid within the cracks was partly displaced onto these surfaces during the air-to-ground compressive loads and during high negative gust loads.

Thus it is probable that in the air plus water spray tests the fatigue cracks were wetted more or less continuously by a solution with enhanced salt content, owing to pick-up from the surfaces, and these conditions increased the environmental influence.

Crack propagation rates

In the data processing the half crack length a (= half the distance between both crack tips) was plotted against the number of flights n, and crack growth delays following severe flights were identified. Crack propagation rates were calculated from the half crack lengths as

$$\frac{da}{dn} = \frac{a_{i+1} - a_i}{n_{i+1} - n_i} \qquad (1)$$

and were related to a half crack length $a^* = (a_{i+1} + a_i)/2$, which is the mean of the crack growth interval.

Crack propagation data for each alloy in each environment are given in figures 3-6. Trend lines have been fitted to the data, and the influences of severe flights together with propagation rate increase-decrease alternations are indicated wherever they might otherwise be considered as data scatter. Figures 3-6 show that for both materials crack propagation rates over the entire range of crack lengths were significantly affected by varying the mean stress level, Smf, although the influence of severe flights was equally important at short crack lengths for 2024-T3. Comparison of figures 3 and 4 and figures 5 and 6 indicates that the effect of Smf was greater for the air plus water spray environment.

Other general points can be made with the help of diagrams like figure 7, which compares trend lines for both materials in both environments at one Smf level. These points are:

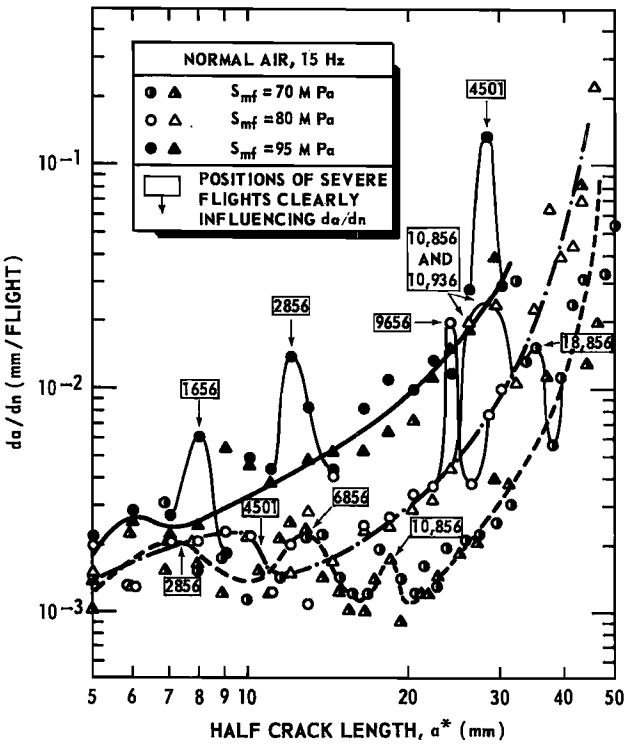

Fig. 3 Crack propagation rates for 2024-T3 in air

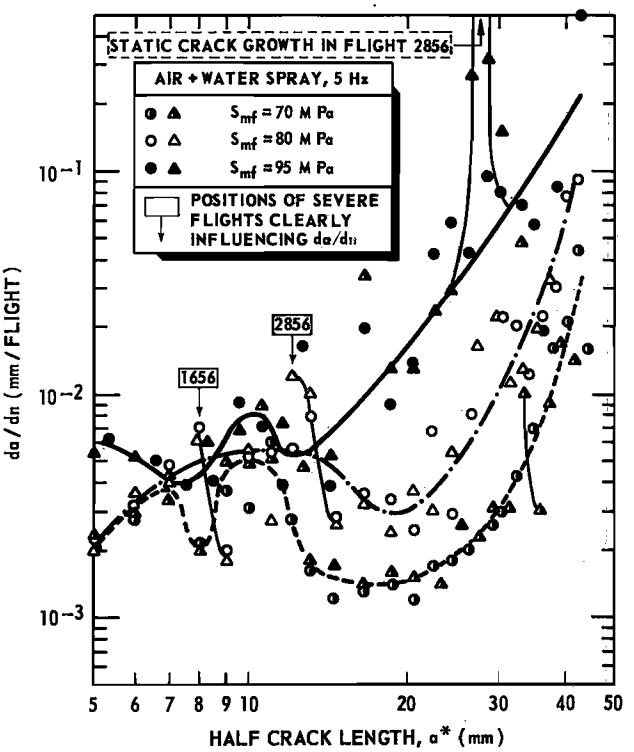

Fig. 4 Crack propagation rates for 2024-T3 in air plus water spray

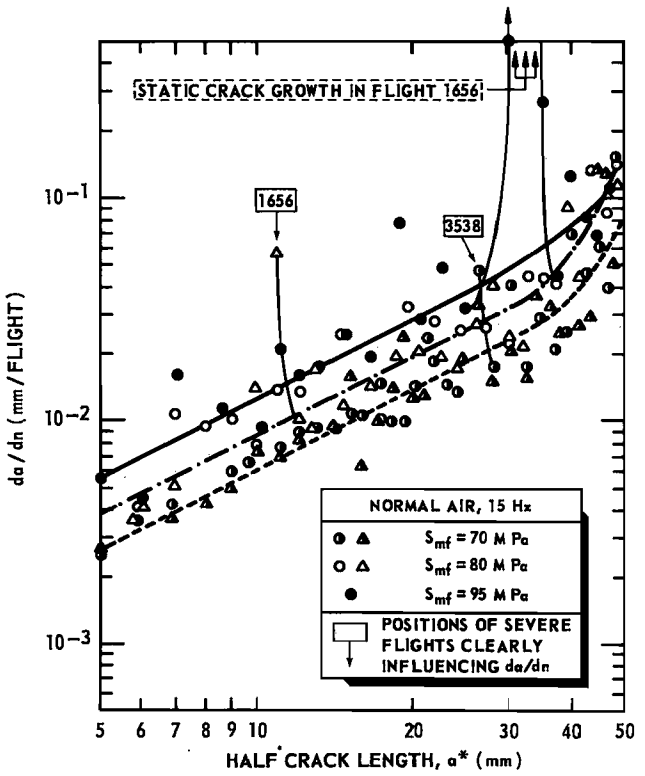

Fig. 5 Crack propagation rates for 7475-T761 in air

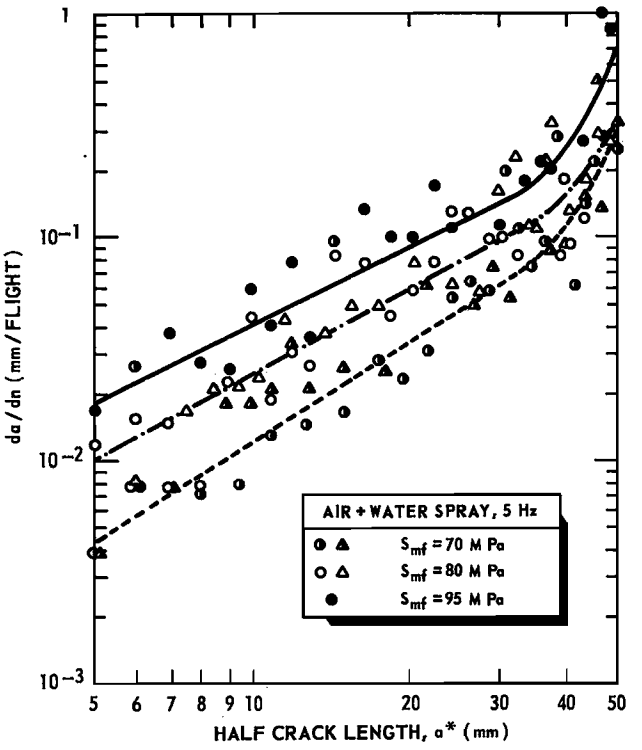

Fig. 6 Crack propagation rates for 7475-T761 in air plus water spray

1) Crack propagation rates for 2024-T3 were accelerated by the air plus water spray environment only at short crack lengths.

2) Crack propagation rates for 7475-T761 were accelerated by the air plus water spray environment at all crack lengths.

3) Severe flights caused large and persistent crack growth retardations for 2024-T3.

4) Crack propagation rates for 7475-T761 were especially higher than those for 2024-T3 over an intermediate range of crack lengths, owing to the occurrence of persistent crack growth retardation for 2024-T3 in this range.

In figures 8-11 the crack propagation rate data have also been plotted against the stress intensity factor Kmf, given by

$$Kmf = Smf \sqrt{\pi a^* \sec\left(\frac{\pi a^*}{W}\right)} \qquad (2)$$

where W is the total width of the specimen and $\sqrt{\sec(\pi a^*/W)}$ is the finite width correction factor suggested by Feddersen [13] for a centre-cracked panel. Figures 8 and 9 show that Kmf does not correlate the 2024-T3 data, owing at least partly to the discrete influence of severe flights. However, a degree of correlation is achieved for 7475-T761, especially for the specimens tested in air, figure 10.

Crack growth delays following severe flights.

From the crack propagation records it was possible to assign some crack growth delays to particular severe flights which preceded and caused them. Extrapolations were made to estimate these delays, which are listed in table 2. The

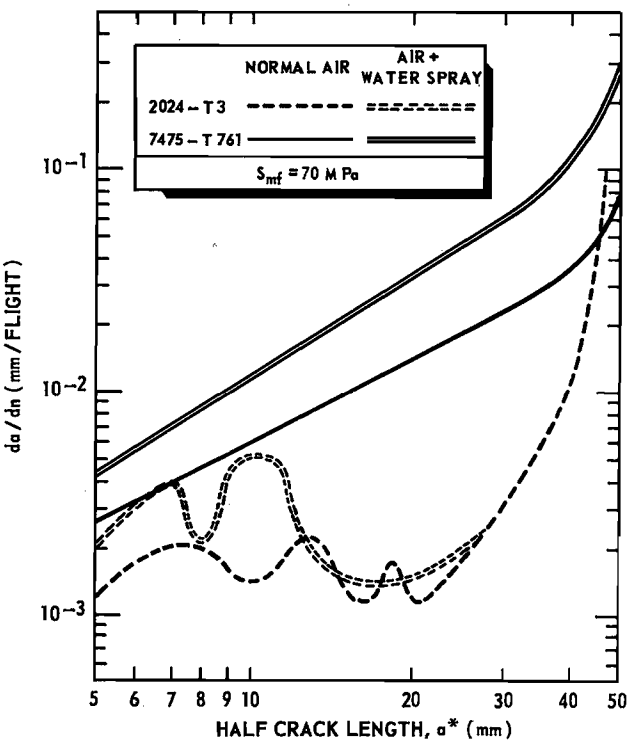

Fig. 7 Comparison of crack propagation curves for 2024-T3 and 7475-T761 with S_{mf}=70MPa

data are limited, but it does appear that:

1) Following the same flight type the delays were longer for 2024-T3 than for 7475-T761, irrespective of Smf level.

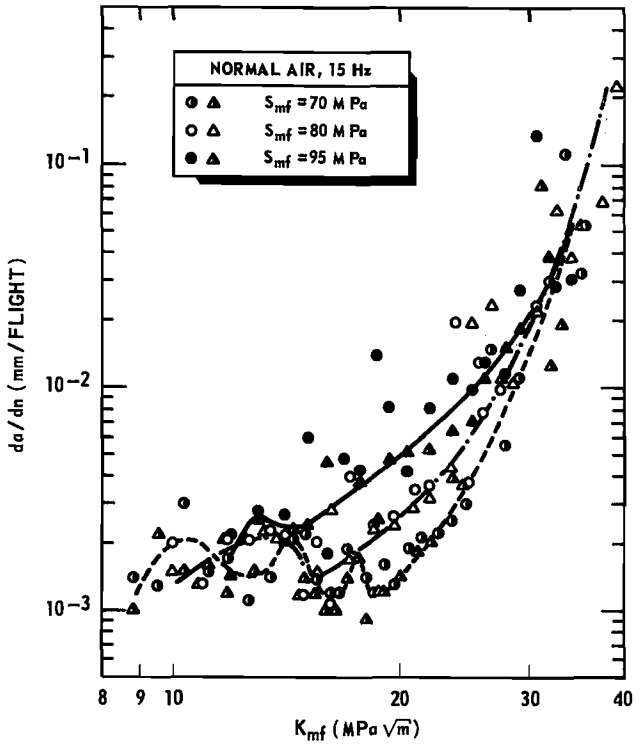

Fig. 8 Crack propagation rates versus K_{mf} for 2024-T3 in air

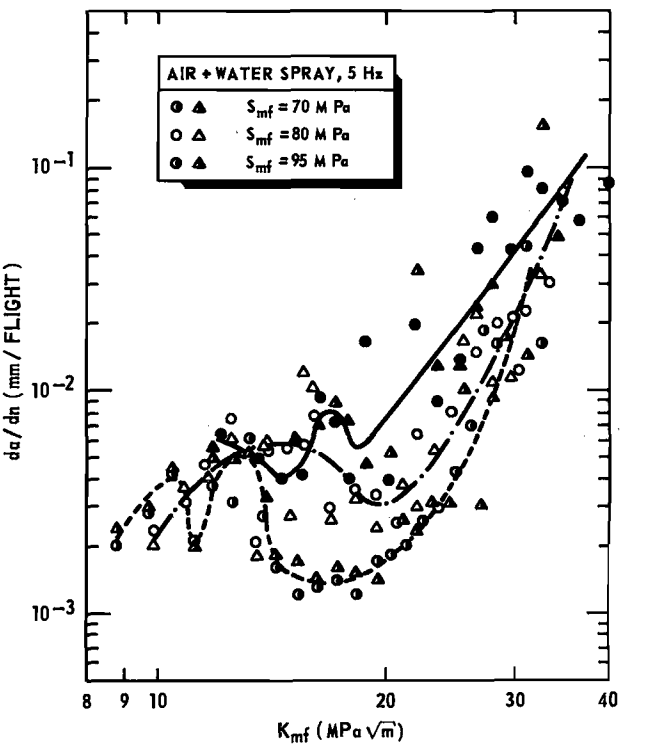

Fig. 9 Crack propagation rates versus K_{mf} for 2024-T3 in air plus water spray

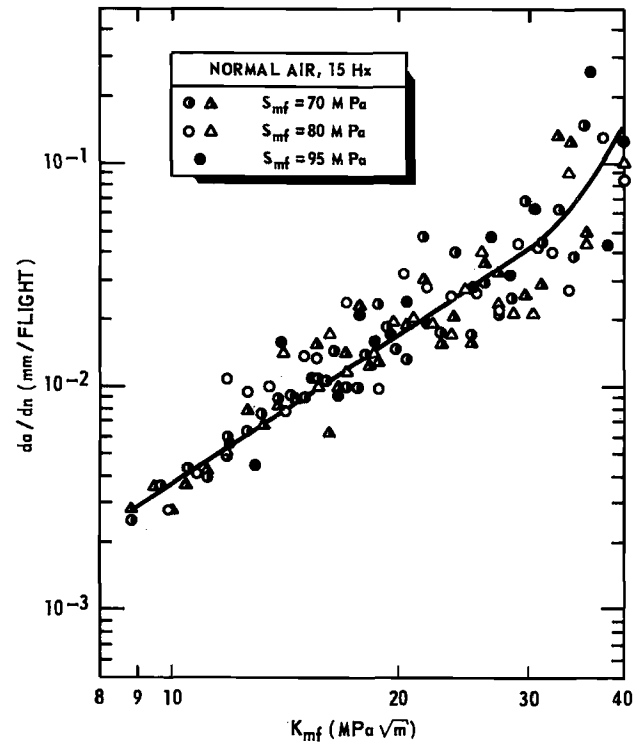

Fig. 10 Crack propagation rates versus K_{mf} for 7475-T761 in air

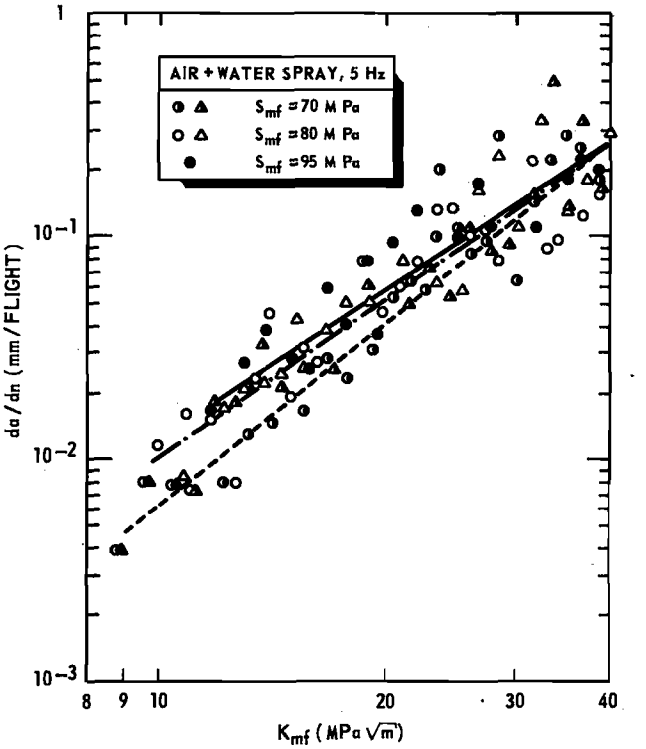

Fig. 11 Crack propagation rates versus K_{mf} for 7475-T761 in air plus water spray

TABLE 2

CRACK GROWTH DELAYS FOLLOWING SEVERE FLIGHTS

material	Smf (MPa)	environment	flight type(s) causing delay	crack length, a, at beginning of delay (mm)	delays (flights)
2024-T3 Alclad	95	air	1656	6.6	210 ; 255
			2856 + 2936	10.3	230 ; 240
		air + water spray	1656	12.1	180 ; 210
			1656	12.2	170 ; 180
7475-T761 bare	70	air	2856 + 2936	16.8	75 ; 75
			2856 + 2936	15.5	75 ; 80
		air + water spray	1656	21.8	60 ; 60
	80	air	1656	12.2	130 ; 130
			1656	10.5	100 ; 100
			2856 + 2936	29.5	75 ; 75
		air + water spray	501	6.7	80 ; 80
	95	air + water spray	501	27.5	15 ; 15

2) For similar crack lengths changing from normal air to an air plus water spray environment resulted in shorter delays. This conclusion is supported by the results for 7475-T761 with Smf = 70 MPa, since the delay for flight 1656, which contained 3 peak loads at level III, was less than the delays for flights 2856 + 2936, which together also contained 3 peak loads at level III.

Discussion

The results of this investigation show that the fatigue crack propagation resistance of 2024-T3 sheet under gust spectrum loading is generally superior to that of 7475-T761 sheet, and that this superiority is mainly due to a greater amount of crack growth retardation during the less severe loads and flights that follow the peak loads in severe flights. Thus the straightforward use of 7475 alloy instead of 2024-T3 in tension-critical structures like the under wing skin of a transport aircraft would result in decreased fatigue crack propagation resistance.

However, fatigue crack propagation resistance depends very much on the structural concept. It should be possible to improve the relative performance of a 7475 alloy structure (in order to utilize the higher static structural efficiency and fracture toughness as compared to 2024-T3) by selecting adhesive bonded laminated sheet or sandwich panel concepts. Significant reductions in crack growth rates can occur owing to load shedding to uncracked laminations [14-16] and uncracked face sheets of sandwich panels [5,17]. Load shedding also has the advantage that a greater amount of the crack propagation life is spent at longer crack lengths, i.e. the inspectability of a load shedding structure is better.

It is evident from recent publications that there is increased interest in laminated [14,15,18-21] and sandwich [3,5,19,20,22-24] structures. But these design options, especially laminates, are likely to be restricted to fairly high load density areas. This is because sheet thicknesses must be sufficient readily to allow manufacture and service use (resistance to denting, scratching, etc.) and therefore it becomes increasingly difficult to save weight the more lightly loaded the structure. Furthermore, the relative weight of adhesive increases for more lightly loaded structures.

It is not known whether the fatigue crack propagation resistance of monolithic 2024-T3 sheet can be equalled or exceeded by laminated or sandwich panels using 7475 alloy at stress levels giving cost-effective weight savings in actual transport aircraft structures. This is a potentially fruitful field for further investigation. In this respect the present results also show that it is important to choose representative simulated conditions of environment, loading history, cycle frequency and stress level. In particular, the environmental influence can be much more significant for flight simulation loading as compared to constant amplitude tests. This is because for loading histories with severe flight peak loads that can cause large crack growth retardations, a more aggressive environment results in basically faster crack growth which not only reduces retardation but also reduces the number of severe flights, and hence retardations, that are encountered.

Finally, the failure of an engineering approach using a characteristic stress intensity factor, Kmf, to try and correlate 2024-T3 data

at different Smf levels is somewhat disappointing. Apparently, a degree of correlation is obtainable only when the discrete influences of severe flights have negligible effect on the crack propagation curve, as was the case for 7475-T761.

Any 7475 alloy structural concept with equivalent crack propagation resistance to that of monolithic 2024-T3 would probably develop an analogous sensitivity to severe flights, and hence attempts to correlate crack growth data by a characteristic stress intensity factor would similarly fail. More hope must therefore be placed in the "second generation" crack propagation models currently being developed [25,26].

Conclusions

1) Straightforward use of 7475 alloy instead of 2024-T3 in tension-critical sheet structures for transport aircraft would result in decreased fatigue crack propagation resistance.

2) In order to utilize the higher static structural efficiency and fracture toughness of 7475 alloy it may be possible to achieve acceptable fatigue crack propagation resistance by selecting adhesive bonded laminated sheet or sandwich panel concepts. However, such concepts are likely to be restricted to areas of fairly high load density.

3) In any test programme for evaluating the fatigue crack propagation resistance of different structural concepts it is important to choose representative simulated conditions of environment, loading history, cycle frequency and stress level.

References

[1] A.C. Ham and A.J. Willshire, J. Roy. Aero. Soc., Vol. 80, p. 434 (1976).

[2] Military Specification MIL-A-83444, USAF, July 1974.

[3] D.G. Smillie and D.M. Purdy, ICAS Paper No. 74-22, The Ninth Congress of the International Council of the Aeronautical Sciences, Haifa, August 1974.

[4] W.A. Pitman and C.R. Bigham, AIAA Paper No. 74-339, AIAA/ASME/SAE 15th Structures, Structural Dynamics and Materials Conference, Las Vegas, April 1974.

[5] J.E. McCarty, AIAA Paper No. 74-340, ibid.

[6] R.J.H. Wanhill, Aluminium, Vol. 54, p. 455 (1978).

[7] R.J.H. Wanhill, Fatigue of Engineering Materials and Structures, Vol. 1, p. 5 (1979).

[8] R.J.H. Wanhill, Paper 2 in Corrosion Fatigue of Aircraft Materials, AGARD Rep. No. 659, October 1977.

[9] W.E. Anderson, International Met. Reviews, Vol. 17, p. 240 (1972).

[10] J.B. de Jonge, D. Schütz, H. Lowak and J. Schijve, NLR TR 73029 U, March 1973.

[11] J.A. Scott, Br. Corros. J., Vol. 6, p. 145 (1971).

[12] R.J.H. Wanhill, F.A. Jacobs and L. Schra, Paper C110/77 in The Influence of Environment on Fatigue, Inst. of Mech. Eng., London, May 1977.

[13] C.E. Feddersen, Discussion in Plane Strain Crack Toughness Testing of High Strength Metallic Materials, ASTM STP 410, p. 77 (1967).

[14] G.F.J.A. van Gestel, Aeronautical Engineers Thesis (in Dutch), Delft University of Technology, April 1975.

[15] R.W. McAnally, AIAA Paper No. 74-338, AIAA/ASME/SAE 15th Structures, Structural Dynamics and Materials Conference, Las Vegas, April 1974.

[16] R.J.H. Wanhill, Fatigue of Engineering Materials and Structures, Vol. 2, p. 319 (1979).

[17] G. Bartelds and A. Nederveen, NLR TR 73129 U, September 1973.

[18] S.W. McClaren and J.R. Ellis, Materials on the Move, Sixth National SAMPE Technical Conference, Vol. 6, p. 345 (1974).

[19] F.A. Figge and L. Bernhardt, AIAA Paper No. 74-337, AIAA/ASME/SAE 15th Structures, Structural Dynamics and Materials Conference, Las Vegas, April 1974.

[20] F.D. Boensch and C.E. Hart, AIAA Paper No. 74-336, ibid.

[21] Aviation Wk. and Space Tech., p. 127, January 26 (1976).

[22] S. Oken and R.R. June, NASA CR-1859, December 1971.

[23] L.L. Bryson and J.E. McCarty, NASA CR-2122, November 1973.

[24] P.L. Sandoz, AIAA Paper No. 73-20, New York (1973).

[25] P.D. Bell and A. Wolfman, Fatigue Crack Growth Under Spectrum Loads, ASTM STP 595, p. 157 (1976).

[26] H.D. Dill and C.R. Saff, ibid., p. 306.